Electronic Supplementary Information

A Biomimetic Molecular Switch at Work: Coupling Photoisomerization Dynamics to Peptide Structural Rearrangement

Cristina García-Iriepa,[⊥‡] *Moussa Gueye,*[‖] *Jérémie Léonard,**[‖] *David Martínez-López,*[⊥] *Pedro J. Campos,*[⊥] *Luis Manuel Frutos,*[‡] *Diego Sampedro,**[⊥] *and Marco Marazzi,**[§†]

[⊥] Departamento de Química, Centro de Investigación en Síntesis Química (CISQ), Universidad de La Rioja, Madre de Dios 53, E-26006 Logroño, Spain

[‡] Unidad Docente de Química Física, Universidad de Alcalá, E-28871 Alcalá de Henares, Madrid, Spain

[‖] Institut de Physique et Chimie des Matériaux de Strasbourg & Labex NIE, Université de Strasbourg, CNRS UMR 7504, 23 rue du Loess, Strasbourg 67034, France

[§] Department of Theoretical Chemical Biology, Institute of Physical Chemistry, KIT, Kaiserstrasse 12, 76131 Karlsruhe, Germany

Contents:

1. Experimental Methods

The TAS set-up is based on a Ti:sapphire generative amplifier laser system, delivering 800 nm, 40 fs pulses at a repetition rate of 5 kHz. A fraction of this fundamental pulse is used for second harmonic generation (SHG in a BBO crystal) to generate a 400-nm pump beam. Another fraction is used to produce a white light probe pulse (supercontinuum generation in CaF_2) covering a spectral range from 290 to > 950 nm. The time delay between pump and probe pulses are adjusted by a stepper motor ("delay line"). The relative linear polarizations of pump and probe beams are set to magic angle (54.7°). The experimental time resolution is ~ 70 fs. The pump intensity is kept in the linear regime of excitation in order to promote the sample to its first excited state (S_1) with a few-percent probability. Both pump and probe beams are focused into a 0.2-mm thick flow cell containing the sample in solution. A peristaltic pump circulates the sample to refresh it between two excitation laser shots. The sample optical density (OD) at the excitation wavelength (400 nm) is 0.3 for compound **1** and 0.05 for compound **2**. For temperature-dependent studies, a thin (1 mm in diameter) temperature gauge was immerged inside the sample reservoir (4 mL), itself inserted in a temperature-stabilized water bath. Quantitative kinetic analysis of the TAS experiments is done by global analysis of the TAS 2D-maps. Singular values decomposition (SVD) is performed for data reduction, and the dominating three singular transients are fitted simultaneously to multiexponential decaying functions convoluted with a Gaussian function representing the instrument response function. Irrespective of the temperatures, the minimal number of time constants required to make a satisfying global fit is of four in the case of ***E*-1** and five for the cross-linked peptide. The results of the global analysis may be disclosed by plotting the Decay-Associated Spectra (DAS) which reveal the wavelength dependence of the pre-exponential amplitudes associated to each decay time constant.

2. Experimental Data.

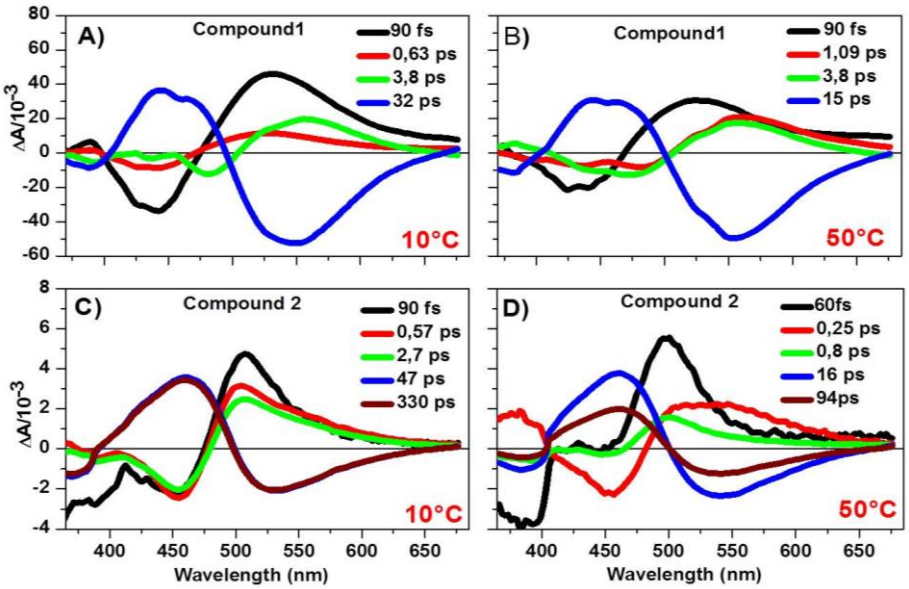

Figure S1: Temperature dependence of the Decay-Associated Spectra (DAS) obtained by global analysis of TAS data of compound **1** (A) at 10°C, (B) at 50°C, and compound **2** (C) at 10°C, (D) 50°C.

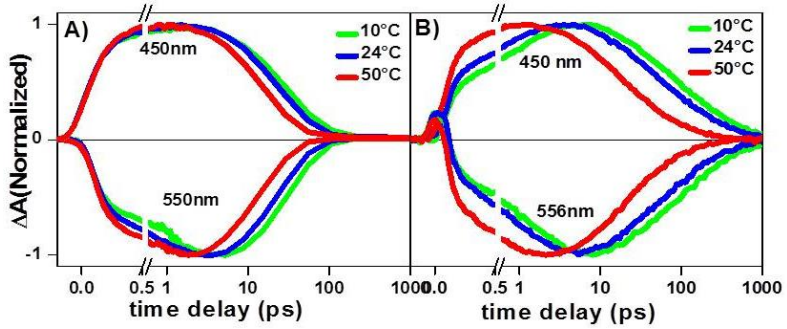

Figure S2: Temperature dependence of the kinetic traces at 450 nm (ESA band, positive curves) and 550 nm (SE band, negative curves) of (A) E-1 and (B) E-2. For compound E-2 (panel B) both the S_1 population relaxation (build up of the signals until their maxima) and S_1 population decay accelerate at higher temperatures.

The temperature dependence of the S_1 decay time constants (τ4 and τ5) of compounds **1** and **2** are analyzed with an Arrhenius law which assumes: $1/\tau = Ae^{-E_A/k_BT}$, with A a pre-exponential factor, E_A the activation energy, k_B the Boltzmann constant. Figure S3 presents the plots of ln(τ) as a function of 1/T and Table S1 presents the results of the linear fits.

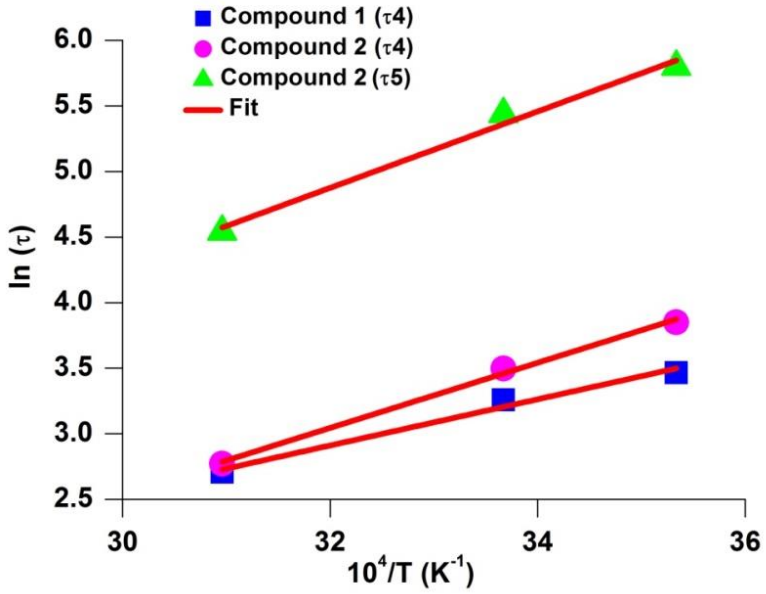

Figure S3: Arrhenius plot (ln(τ) as a function of 1/T) illustrating the temperature dependence of the S_1 lifetimes of compound **1** (τ4), and of **2** (τ4 and τ5). Red lines are linear fits (see Table S1).

Table S1. Result of the linear fit of the Arrhenius plots above (Figure S3).

	Compound **1**, τ4	Compound **2**, τ4	Compound **2**, τ5
A (ps-1)	15 (7 to 30)	130 (80 to 220)	85 (30 to 220)
E_A/k_B (K) E_A (kcal·mol^{-1})	1760 +/- 200 3.5	2480 +/- 150 4.9	2910 +/- 300 5.8

3. Computational Details.

In order to study the peptide conformational changes, the bare peptide and the cross-linked peptide (compounds ***E*-2** and ***Z*-2**) were placed in a cubic box with side length 67.6913 Å, 66.8257 Å and 66.7747 Å, respectively. Then, the boxes were filled with water molecules represented by the TIP3P model[1] (10140, 9709 and 9696 water molecules, respectively).

We used the AMBER99SB force field[2] for the peptide and the generalized AMBER force field (GAFF[3]) for the switch. Because of the thermal stability of separated *E* and *Z* isomers at 300 K,[4] charges have been calculated for both *E* and *Z* isolated molecules at the Hartree–Fock level of theory in the framework of the Merz–Singh–Kollman scheme,[5,6] after geometry optimization with the B3LYP[7] functional. The generated MM switch parameters were validated by calculating a scan around the isomerizable formal double bond at the GAFF and MP2 level (see Figure S4). Moreover, a chloride anion was added to get a neutralized system.

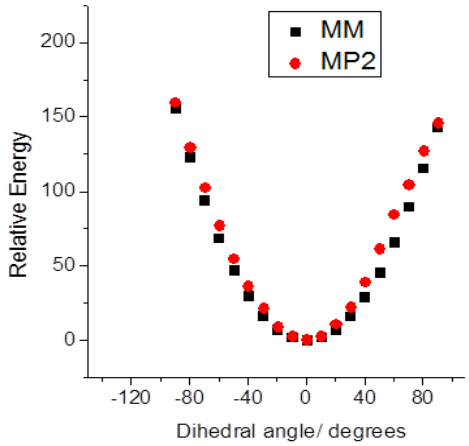

Figure S4. Ground state energy scan around the isomerizable C=C double bond (*E* isomer) at the MM and MP2 level of theory.

Regarding compound **1** in MeOH, the model system was placed in a cubic box of initial size 4.699 × 4.699 × 4.699 Å containing 395 solvent molecules. The switch was treated as previously described and again, a chloride anion was added to electroneutralize the model. For comparison with ultrafast spectroscopy experiments, a simplified model of **1** was embedded in an explicit cubic box of MeOH molecules. The simplification consists in replacing the ^{t}Bu group of each BOC (*tert*-butyloxycarbonyl) moiety with a methyl group. This structural modification reduces the computational time and should have almost no effect on the photochemistry since the chromophore stays intact. Again, the switch has been represented by the GAFF, while methanol molecules are modeled by a force field developed by Dang et al.[45] Since the interest related to the photoswitch **1** in MeOH concerns mainly its photochemistry (*i.e.* no conformational study is needed), this model was equilibrated in the canonical (NVT) and isothermal-isobaric (NPT) ensembles (300 K, 1 atm) without calculating additional MD trajectories.

All studied systems were first equilibrated in the isotherm (NVT) and isobar (NPT) ensembles to reach a temperature of 300 K and a pressure of 1 atm, before running the production dynamics (not required for compound **1**).

The optimized model **1** and 50 MD snapshots of the ***E*-2** and ***Z*-2**, were extracted to calculate the electronic vertical transitions at the time dependent (TD-)DFT/MM level of theory, after calibration with the multiconfigurational MS-CASPT2//SA-2-CASSCF/MM level of theory. The selected criterion to extract MD snapshots was the sulphur-sulphur distance (spanning *ca.* 10 Å for both isomers), which was found to be of particular relevance for conformational analysis. Finally, the absorption spectra were built as a convolution of Gaussian functions.

QM/MM models were built for the simplified compound **1** and compound **2**. More precisely, while the QM/MM frontier does not involve any covalent bond for the simplified compound **1** (the switch is entirely in the QM region, surrounded by MeOH solvent molecules in the MM region), two hydrogen link atoms (HLAs) are needed to treat the boundaries between the switch and the rest of the peptide on compound **2**. The HLAs are therefore placed along the C-C single bonds connecting the cysteine residues to the C=O moieties of the switch (see Figure 1B in the main text), and the Morokuma scheme is applied to keep the HLAs aligned during QM/MM optimizations and non-adiabatic dynamics.[8]

Combined with the molecular mechanics force field, the Møller–Plesset perturbation theory to the 2nd order (MP2) was used to optimize structures on the electronic ground state. The MP2/MM optimized structures of model **1** and of two most significant ***E*-2** conformers, were considered as starting geometries for the calculation of the *E*-to-*Z* minimum energy paths (MEPs) at the SA-2-CASSCF level. Along the MEP calculations, a radius of 15 Ångstroms around the molecular switch (QM region) is allowed to optimize at the MM level, including water molecules, peptide backbone and side chains.

The State Averaged-Complete Active Space Self Consistent Field (SA2-CASSCF) was used to calculate minimum energy paths and non-adiabatic dynamics, including the electronic ground state and the first two excited states, averaged with equal weights. The active space selected was 12 electrons in 12 orbitals (see Figure S5). The step size used in the MEP simulations was 0.1 a.u. (in normalized mass-weighted coordinates) for all calculations. The conical intersections were characterized by calculating the non-adiabatic coupling vectors (i.e. derivative coupling (DC) and gradient difference (GD) vectors), in order to determine the S_1/S_0 crossing topology. The Multi State-Complete Active Space Perturbation Theory to the 2nd order (MS-CASPT2) method was used to correct the SA-CASSCF energies, including an imaginary shift of 0.2 and no IPEA shift.

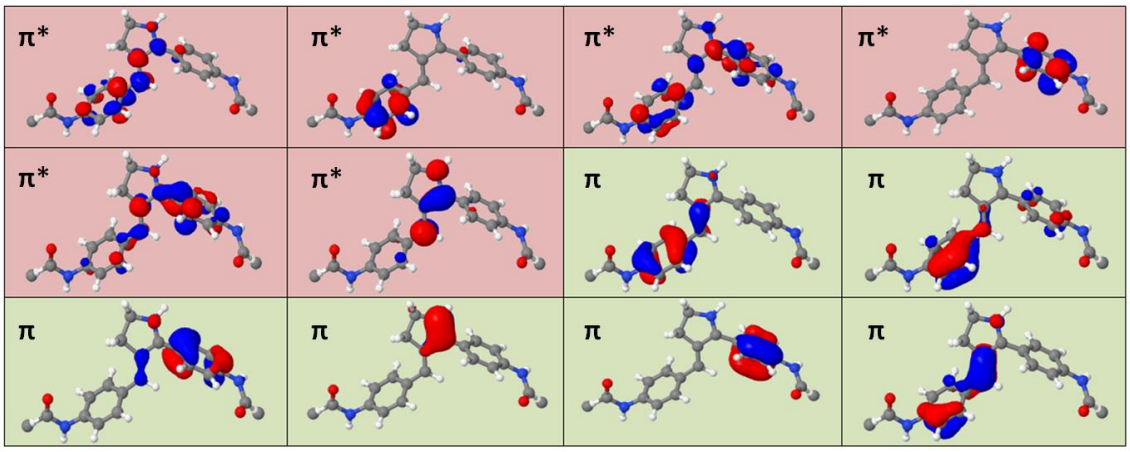

Figure S5. π* and π orbitals included in the active space used for CASSCF and CASPT2 calculations.

4. Electronic Transitions of the Simplified Compound 1.

The optical bright state is the first singlet excited state S_1. The excitation energies calculated for both, the equilibrated (NVT and NPT) and the S_0 optimized structures (after equilibration), are in very good agreement with the experimental one (Table S2). The electronic transition is described by the excitation of one electron from the HOMO to the LUMO (see Figure S6). The HOMO orbital is a π orbital centered in the photoisomerizable CC double bond and also on one phenyl ring. Whereas, the LUMO is a π* orbital centered in the same CC double bond and partially in the C=N bond of the five membered ring.

Table S2. CASPT2/MM and TD-DFT/MM vertical transitions energies, electronic nature and oscillator strengths (f) for the switch in MeOH.

	Level of theory	**State**	**E_{CASPT2} / eV (nm)**	**f**
Optimized structure	CASPT2 (12,12)/AMBER 6-31G*	S_1 (π→π*)	3.09 (401)	1.1346
Equilibrated Structure	CASPT2 (12,12)/AMBER 6-31G*	S_1 (π→π*)	3.12 (398)	0.9897
	TD-DFT/AMBER 6-311+G(d,p) (M062X)	S_1 (π→π*)	3.24 (383)	1.2479

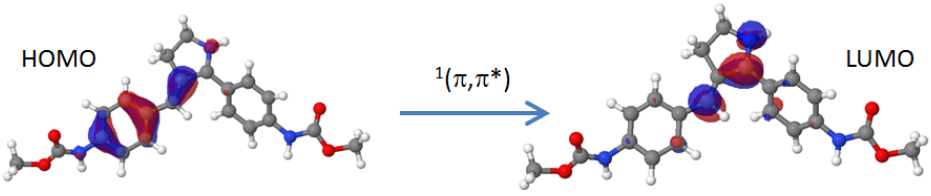

Figure S6. CASSCF molecular orbitals describing the electronic nature of the optically bright state of compound **1**.

5. MD Analysis.

As described in the main text, 10 MD simulations were run for compounds ***E*-2** and ***Z*-2**. Some key parameters were analyzed for each trajectory as the SS distance and the distribution of the dihedral angles φ_E and φ_Z. The first parameter is important in order to measure the change in end-to-end length of the photoswitch after isomerization. Regarding the dihedral analysis, we check that both isomers do not interconvert along the simulation, that is, no thermal isomerization is taking place. We select one representative simulation to illustrate these analyses. The SS distance and the φ_E and φ_Z distributions are shown in Figures S7 respectively.

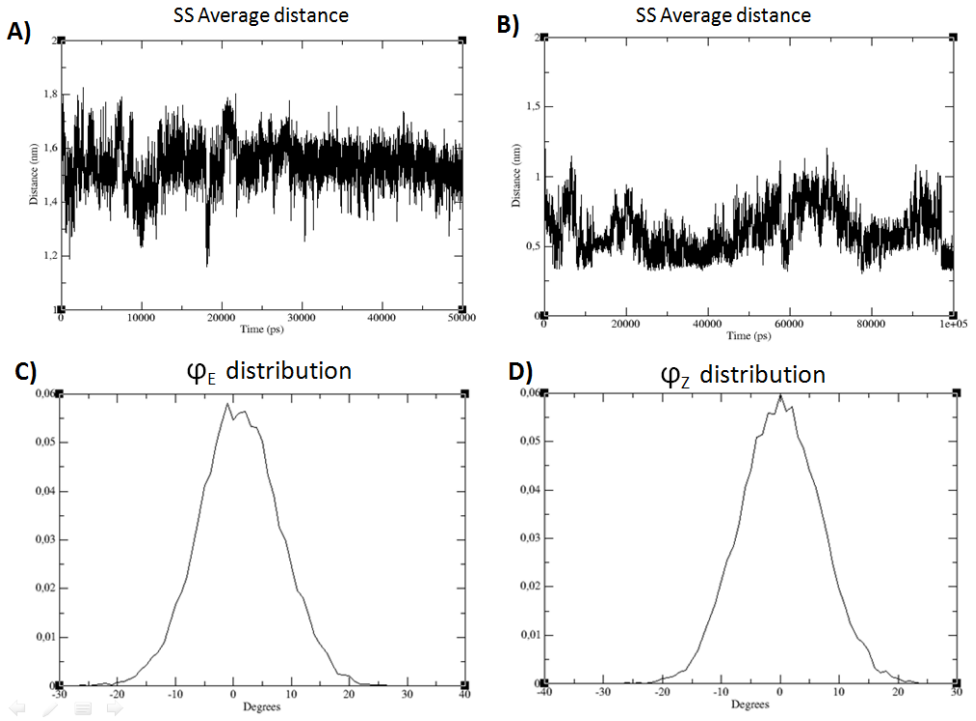

Figure S7. SS average distance analysis along time (50 ns, corresponding to one of the 10 MD simulations performed) for the peptide cross-linked with the A) *E* isomer and B) *Z* isomer. Distribution of one of the dihedral angles involved in the photoisomerization for the peptide cross-linked with the C) *E* isomer and D) *Z* isomer.

Then, a cluster analysis for the bare peptide and the peptide cross-linked with the *E* isomer was performed in order to check the system heterogeneity in the ground state. With this aim, average structures of the peptide conformations were calculated using the "g_cluster" tool of GROMACS. The gromos method and a backbone root mean square deviation (RMSD) cutoff of 0.47 nm were selected. With these criteria, 31 and 39 clusters were found respectively but, in both cases, only two of them are the main ones (population >10%, Table S3). Moreover, for both systems one cluster structure is characterized by a larger SS average distance (see Table S3).

Table S3. Cluster analysis for the bare peptide and the *E* isomer cross-linked peptide. The number of structures, percentage and SS average distance are detailed.

System	Nº Cluster	Nº Structures	%	SS average distance (Å)
Bare peptide	1	8954	55	16.0
	2	3256	20	14.4
	3	1302	8	16.4
	4	847	5	16.8
	5	423	2	17.5
	6	286	2	19.9
	7	248	1	19.5
	8	197	1	22.3
	9	177	1	11.3
***E* isomer cross-linked peptide**	1	8140	50	14.7
	2	2605	16	11.5
	3	1139	7	13.3
	4	746	4	15.5
	5	561	3	11.0
	6	513	3	16.6
	7	419	2	14.0
	8	334	2	11.3
	9	332	2	17.0
	10	261	1	14.9
	11	170	1	13.6

6. Absorption Spectra of *E*-2-C1 and *E*-2-C2.

The *E* isomer ground state is structurally heterogeneous and two main conformations have been found (see MD analysis), denoted cluster 1 (C1) and cluster 2 (C2). We have simulated the absorption spectra for different snapshots of each cluster at the MS-CASPT2//SA2-CASSCF/MM level of theory. The optically bright state is the first singlet excited state S_1. The spectra of both clusters are shown in Figure S8. They are nearly identical, equally broad, and centered around 380-390nm, indicating that both clusters are not spectroscopically distinguishable. The experimental spectrum shows a broad band with its maximum around 375 nm.

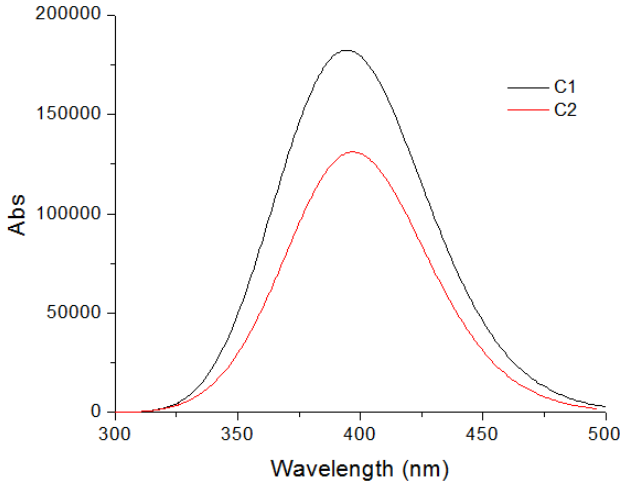

Figure S8. Absorption spectra simulated for both clusters, C1 and C2 of the *E* isomer.

7. Absorption Spectra Calibration: TD-DFT/MM vs. CASPT2/MM .

We simulated the absorption spectrum for 10 snapshots of each the *E* and the *Z* isomer cross linked peptide (20 snapshots total) at the MS-CASPT2//SA2-CASSCF/MM level of theory. This method is computationally expensive so we use it as a benchmark to assess the accuracy of the spectra computed from the same snapshots at the TD-DFT/MM level of theory using the M062X functional. The results are displayed in Figure S9. At the TDDFT/MM level, both spectra are blue shifted of around 20 nm but, the nature of the electronic transition and the relative intensities are in agreement. Therefore, we decided to increase the statistic up to 50 snapshots for each system and calculate the spectra at the TDDFT/MM level of theory, computationally less expensive (Figure 2C in the main text).

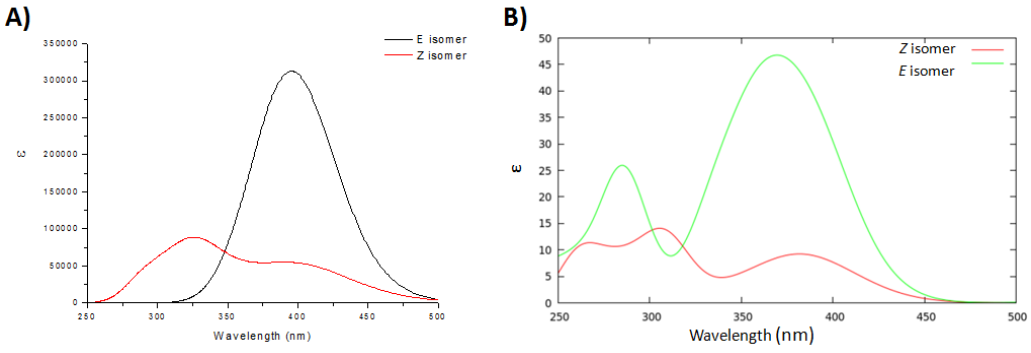

Figure S9. Absorption spectra of 10 snapshots for the *E* and *Z* isomer cross linked peptide at the A) MS-CASPT2//SA2-CASSCF/MM and B) TD-DFT/MM level of theory.

8. Minimum Energy Paths for *E*-2-C1 and *E*-2-C2.

The minimum energy paths were calculated for C1 and C2 at the SA2-CASSCF(12,12)/MM. The photochemistry of both clusters is found to be very similar. From the Franck–Condon structure the system minimizes the energy by activation of the stretching mode (elongation of the C=C bond) reaching an almost planar minimum in S_1 (Figure S10). From there, the system has to

overcome an energy barrier of 8.48 and 5.22 kcal·mol^{-1} at the SA2-CASSCF/MM level of theory. Once reached the TS structure the system can evolve minimizing the energy along the torsion coordinate upon reaching the conical intersection with the ground state, S_0. Two main paths are possible after the decay to the ground state, internal conversion of photoproduct formation (Figure S11).

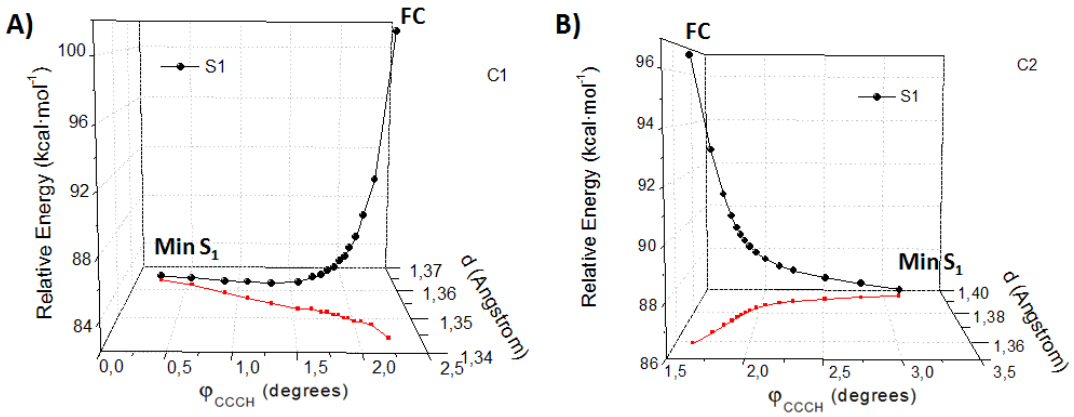

Figure S10. MEP from the FC structure to the minimum in S_1 for A) ***E*-2-C1** and B) ***E*-2-C2**.

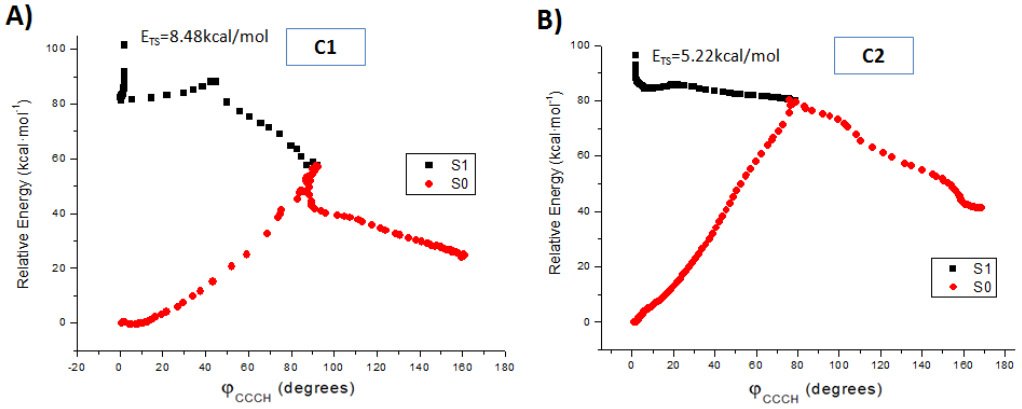

Figure S11. Minimum energy paths for A) ***E*-2-C1** and B) ***E*-2-C2**.

Moreover, the structural changes of the C1 conformer along the MEP, including the effects on the amino acids in the vicinity of the molecular switch, are shown in Figure S12.

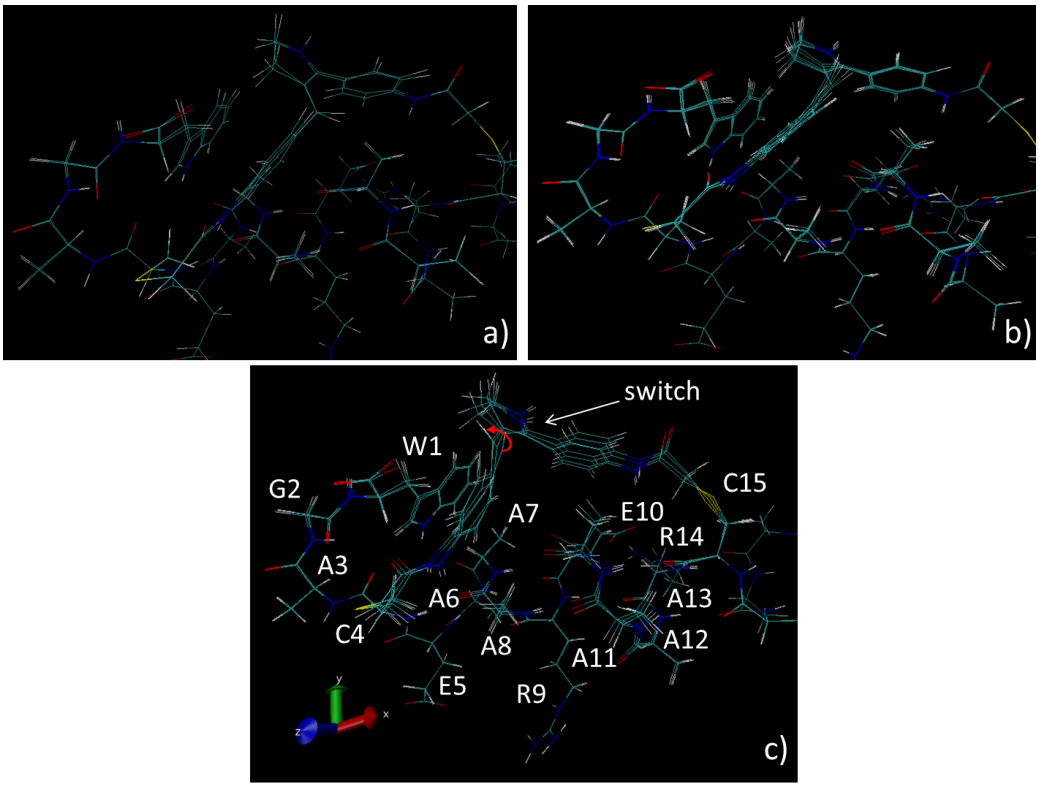

Figure S12. Structural changes of the C1 conformer along the calculated MEP, including the molecular switch and the first 15 amino acids of the peptide sequence: a) from S_1 minimum to S_1 TS; b) from S_1 TS to S_1/S_0 CI; c) photoisomerization path from $S_0 \rightarrow S_1$ vertical excitation to S_1/S_0 CI. The red arrow indicates the isomerizing bond.

Finally, a structural comparison between E-1, E-2-C1 and E-2-C2 is given in Table S4, in terms of the main geometrical parameters of the molecular switch along the S_1 pathway.

Table S4. Structural comparison between E-1, E-2-C1 and E-2-C2 along the photoreaction pathway.

	***E*-1**			***E*-2-C1**			***E*-2-C2**		
	S_1 FC	S_1 min	S_1 TS	S_1 FC	S_1 min	S_1 TS	S_1 FC	S_1 min	S_1 TS
$d_{C-C} - d_{C=C}$ (Å)[i)]	0.11	0.002	-0.04	0.14	0.11	0.03	0.09	0.05	-0.06
φ_{CCCC} (°)	2.9	7.7	16.3	1.5	4.2	35	11.4	13.0	40
φ_{CCCH} (°)	-0.4	1.9	30	2.2	0.2	45	1.6	3.1	20
Pyramidalization of the PSB nitrogen atom (°)	2.6	12.2	11.2	2.1	0.7	45	4.8	13.2	25
Charge transfer character[ii)]	0.59	0.60	0.57	0.83	0.88	0.88	0.68	0.67	0.52
S_1 energy barrier[ii)]	3 kcal·mol^{-1}			13 kcal·mol^{-1}			5 kcal·mol^{-1}		
S_0 SS average distance (Å)	-			14.7	-	-	11.5	-	-

[i)] the difference between single and double bond lengths quantifies the so-called "Bond Length Alternation" (BLA) deformation: when this becomes <0, the double bond acquires single bond character which enables torsional motion around φ_{CCCC}.

[ii)] the charge transfer character is calculated by splitting the chromophore in two fragments at the vinyl CH moiety (see Figure 2D) . The numbers in that line of the table are the charge predicted to sit on the six-membered ring directly bound to the photoisomerizable C=C bond.

iii) predicted from the 1D (E-1) or 2D (E-2, see figure 9) PES sampling at the CASPT2 level, see below.

9. CASPT2//CASSCF Energy Profile of the Molecular Switch in MeOH, C1 and C2 in H_2O.

Single point energy corrections at the MS-CASPT2 level have been done along the minimum energy path calculated at the SA2-CASSCF/MM level of theory for the three systems under study: *E* isomer in MeOH and the *E* and *Z* isomer cross-linked peptide in water. As observed in Figure S13, a good agreement between CASSCF and CASPT2 relative energies and TS energies is found.

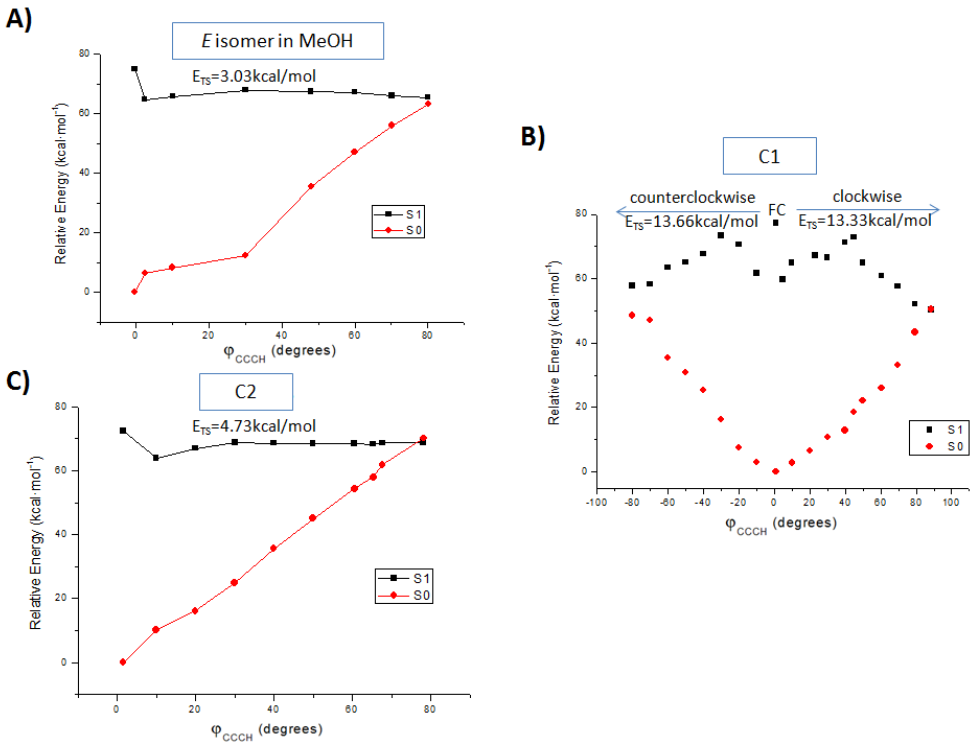

Figure S13. CASPT2 single energy corrections along the CASSCF minimum energy paths of the A) *E* isomer in MeOH, B) ***E*-2-C1** and C) ***E*-2-C2**.

10. Cartesian Coordinates of the Most Relevant Optimized Structures.

FC STRUCTURE *E*-1

C	9.20342	-1.40876	2.67527
H	8.99285	-2.11418	3.46586
H	9.48754	-1.94103	1.77917
H	9.98752	-0.73293	2.97513
O	8.06971	-0.59306	2.42904
C	6.97153	-1.19677	2.00516
O	6.87976	-2.37161	1.80799
N	5.99135	-0.27056	1.83716
H	6.24107	0.65568	2.10482
C	4.67054	-0.46183	1.41829
C	4.19497	-1.63723	0.85163
C	2.87889	-1.72813	0.43930
H	2.56352	-2.64928	-0.00534
H	4.85078	-2.47345	0.73273
C	3.80062	0.62657	1.55379
H	4.15526	1.55027	1.97264
C	2.48337	0.52257	1.14830
H	1.83932	1.37543	1.26150
C	1.98476	-0.65994	0.58050
C	0.57762	-0.65815	0.17120
H	0.05947	0.24415	0.43769
C	-0.15899	-1.57897	-0.49047
C	0.19185	-2.96904	-0.99749
H	0.86838	-2.91336	-1.84129
H	0.65489	-3.57359	-0.23265
C	-1.15834	-3.57883	-1.41358
H	-1.50025	-4.35749	-0.74699
H	-1.18316	-3.94551	-2.42718
N	-2.07695	-2.43673	-1.30574
H	-3.02432	-2.48161	-1.63366
C	-1.57007	-1.35743	-0.80962
C	-2.38705	-0.14325	-0.64673
C	-1.92898	1.09354	-1.10905
C	-2.77092	2.19459	-1.07228
H	-2.42599	3.13738	-1.44933
H	-0.95170	1.19318	-1.54124
C	-3.68046	-0.23535	-0.12025
H	-4.03247	-1.16733	0.28022
C	-4.51068	0.85950	-0.07123
H	-5.49671	0.76897	0.33371
C	-4.06925	2.08594	-0.56818
N	-4.86515	3.23591	-0.56216
H	-4.39860	4.11495	-0.59816
C	-6.21972	3.27882	-0.70424
O	-6.94304	2.33132	-0.76234
O	-6.61474	4.53526	-0.77354
C	-8.00234	4.76652	-0.98247
H	-8.29274	4.41992	-1.96261
H	-8.58943	4.26139	-0.23230
H	-8.12838	5.83308	-0.90794

MINIMUM S_1 *E*-1

C	9.19432000	-1.30633000	2.73441000
H	9.00868000	-2.11668000	3.42506000
H	9.52506000	-1.69616000	1.78226000
H	9.92106000	-0.62195000	3.13896000
O	8.00622000	-0.53466000	2.56256000
C	6.96496000	-1.12872000	2.03417000
O	6.90800000	-2.25503000	1.66274000
N	5.91964000	-0.21723000	1.99381000
H	6.14322000	0.67706000	2.37908000
C	4.67718000	-0.36679000	1.47843000
C	4.21989000	-1.52591000	0.80721000
C	2.94290000	-1.58024000	0.34935000
H	2.64373000	-2.45022000	-0.19667000
H	4.89054000	-2.34218000	0.64661000
C	3.78929000	0.74471000	1.63441000
H	4.15095000	1.64472000	2.09502000
C	2.49798000	0.67037000	1.18567000
H	1.85157000	1.51757000	1.30902000
C	1.99298000	-0.50679000	0.54855000
C	0.62572000	-0.51973000	0.16297000
H	0.09830000	0.37973000	0.41263000
C	-0.15008000	-1.50603000	-0.49880000
C	0.23024000	-2.93490000	-0.86008000
H	0.86095000	-2.94506000	-1.74432000
H	0.75984000	-3.44156000	-0.06534000
C	-1.11620000	-3.63089000	-1.14212000
H	-1.39454000	-4.29793000	-0.33100000
H	-1.10549000	-4.20852000	-2.05787000
N	-2.04539000	-2.52820000	-1.23942000
H	-2.91645000	-2.60228000	-1.71702000
C	-1.52016000	-1.32956000	-0.85870000
C	-2.36849000	-0.15322000	-0.74946000
C	-1.91266000	1.13934000	-1.06670000
C	-2.77571000	2.22190000	-1.02306000
H	-2.41581000	3.19794000	-1.28924000
H	-0.90694000	1.29401000	-1.41001000
C	-3.71702000	-0.28922000	-0.36806000
H	-4.08841000	-1.25637000	-0.09016000
C	-4.57198000	0.78584000	-0.30821000
H	-5.59084000	0.64410000	-0.01256000
C	-4.11351000	2.05755000	-0.64686000
N	-4.92183000	3.20137000	-0.60709000
H	-4.45818000	4.08117000	-0.56351000
C	-6.26669000	3.26016000	-0.79819000
O	-6.99957000	2.32927000	-0.94162000
O	-6.65472000	4.52476000	-0.80144000
C	-8.03521000	4.77281000	-1.02311000
H	-8.31328000	4.46967000	-2.02120000
H	-8.63792000	4.24084000	-0.30374000
H	-8.15802000	5.83594000	-0.90581000

TS S_1 *E*-1

C	9.18155200	-1.22689100	2.59737500
H	9.03594900	-2.09055500	3.22770700
H	9.49513000	-1.53431700	1.61209200
H	9.90257500	-0.55776500	3.03451200
O	7.97141300	-0.47717300	2.51633800
C	6.93660300	-1.05265800	1.95518900
O	6.90343100	-2.14632400	1.49643000
N	5.86755600	-0.17203300	2.01028100
H	6.06554100	0.68050300	2.49072300
C	4.61905300	-0.31046100	1.50110000
C	4.20025700	-1.39116600	0.68932800
C	2.91386600	-1.45087200	0.25900000
H	2.63527100	-2.25489700	-0.38910500
H	4.90469600	-2.14153900	0.40268300
C	3.68948300	0.72937900	1.81912900
H	4.02280000	1.57924800	2.38335700
C	2.38621200	0.63815400	1.42167800
H	1.69858700	1.41786300	1.68825400
C	1.91495300	-0.47963200	0.65362900
C	0.53747100	-0.56730700	0.38500000
H	-0.06642800	0.14677300	0.91311600
C	-0.21165700	-1.58294600	-0.32685200
C	0.20763300	-2.99545400	-0.69946000
H	0.88992100	-2.98170100	-1.54627200
H	0.69097300	-3.52191800	0.11144800
C	-1.11843500	-3.66921900	-1.09851100
H	-1.49737600	-4.29865700	-0.29900200
H	-1.03319100	-4.27384200	-1.99007300
N	-2.00471500	-2.54725800	-1.31683100
H	-2.81518100	-2.60130800	-1.89222500
C	-1.49940200	-1.36729700	-0.86596900
C	-2.34718900	-0.18039800	-0.79219000
C	-1.85544800	1.11265800	-1.02877700
C	-2.70786700	2.20411100	-0.99981300
H	-2.32068100	3.18397100	-1.20451800
H	-0.82313400	1.26637200	-1.28094600
C	-3.71451900	-0.31457500	-0.50050900
H	-4.11220800	-1.28646000	-0.28501800
C	-4.56040800	0.76989000	-0.44708400
H	-5.59563900	0.63078500	-0.21721100
C	-4.06861200	2.04487200	-0.71055800
N	-4.86315900	3.19784800	-0.67861900
H	-4.39138800	4.07175400	-0.60838900
C	-6.20902700	3.27598100	-0.85781200
O	-6.95355400	2.35698800	-1.01811400
O	-6.58370600	4.54404100	-0.82943800
C	-7.96269200	4.81088000	-1.04053200
H	-8.24892700	4.52918900	-2.04222600
H	-8.56872000	4.27182200	-0.32943700
H	-8.07438100	5.87330300	-0.90395300

FC STRUCTURE *E*-2-C1

C	33.01085700	39.55380500	35.91936900
C	18.55260200	36.71233600	39.09524800
C	19.83638600	37.38397300	39.50205700
O	20.23072000	37.32112000	40.63159300
N	20.45220000	38.01458600	38.47505000
C	21.63144800	38.77729900	38.43527700
C	21.95996700	39.35259900	37.21498200
C	22.47367700	38.96735900	39.53474300
C	23.62654900	39.73540200	39.37825000
C	23.96400400	40.30433600	38.14384200
C	23.11066500	40.09507800	37.05702500
C	25.20171600	41.11289600	37.96355400
C	25.38323100	42.34762700	38.46185900
C	24.46508100	43.20119400	39.31486400
C	25.01450900	44.62495900	39.12193800
N	26.34787600	44.37756600	38.53501800
C	26.56213800	43.17161700	38.17070600
C	27.84017500	42.74467600	37.55860800
C	28.19879900	43.13100300	36.27001100
C	29.40839800	42.70686000	35.73022000
C	30.27055000	41.91813400	36.46656800
C	29.92158100	41.55487600	37.77745500
C	28.71211900	41.95578000	38.31483800
N	31.41320400	41.37356600	35.84457100
C	32.45008200	40.80654300	36.52044300
O	32.80591700	41.15891800	37.62290200
H	27.05837700	45.09047300	38.45237900
H	21.28632200	39.24000500	36.38364100
H	23.33508300	40.53214100	36.10012400
H	24.25938600	39.90192700	40.22991400
H	22.20510400	38.57324100	40.49077200
H	25.97974600	40.69630800	37.34750000
H	24.54531000	42.90854300	40.35213600
H	23.42859700	43.10898300	39.02928700
H	25.13015200	45.17411100	40.04338800
H	24.44067100	45.22385200	38.42791800
H	28.44710000	41.64984000	39.30950800
H	27.53995600	43.73493600	35.67415100
H	29.66676600	42.98441600	34.72448800
H	30.57134400	40.94535900	38.36765800
H	31.33598600	41.15056300	34.87050100
H	19.96374700	37.95268700	37.61126400
H	32.86158900	39.88726100	36.07936400
H	18.89432200	36.89111400	39.20353300

MINIMUM S_1 *E*-2-C1

C	33.01090194	39.55385177	35.91897225
C	18.55588060	36.71458059	39.09886137
C	19.83697405	37.38166481	39.51691746
O	20.24028581	37.32957088	40.62722491
N	20.48280180	38.03824564	38.46575399
C	21.61118957	38.76966856	38.42980438
C	21.95513896	39.35454957	37.17879078
C	22.48073278	38.96810164	39.55846961
C	23.63142431	39.70873885	39.39947172
C	23.97619870	40.31099594	38.16607188
C	23.07641809	40.09741620	37.05382775
C	25.20601818	41.09345442	37.97472696
C	25.41012923	42.36269944	38.43131700
C	24.48131949	43.21002143	39.29524286
C	25.02960894	44.64325981	39.11611204
N	26.34792890	44.42063668	38.55891014
C	26.53080362	43.14483523	38.15717300
C	27.81725394	42.73280604	37.55548873
C	28.19737408	43.12131062	36.27154329
C	29.41318990	42.70986866	35.73295037
C	30.27282804	41.91938515	36.46742877
C	29.91950444	41.54978998	37.77163727
C	28.70842784	41.95595848	38.30521800
N	31.42108291	41.37276930	35.84328354
C	32.45242286	40.80797835	36.51857014
O	32.81000895	41.15572006	37.62361013
H	27.06244795	45.11299947	38.48078259
H	21.27688224	39.23842571	36.35632761
H	23.32476750	40.54198921	36.10851150
H	24.26879807	39.88244715	40.24196810
H	22.19685190	38.57642387	40.51033675
H	25.96604616	40.64989223	37.35583775
H	24.55782182	42.90101004	40.33302369
H	23.43749408	43.12581792	39.02119086
H	25.10057717	45.17983649	40.05211033
H	24.41760338	45.22630797	38.43422588
H	28.44441306	41.65505036	39.30219217
H	27.53930755	43.72858632	35.67809401
H	29.67253150	42.98792202	34.72666301
H	30.57354104	40.94686040	38.36561374
H	31.33813439	41.14217916	34.87263505
H	19.98498254	37.96805885	37.60344204
H	32.86224470	39.88767807	36.07857460
H	18.89688500	36.89214661	39.21014050

TS S_1 *E*-2-C1			
C	32.98994500	39.52714300	35.92079800
C	18.58495500	36.74879900	39.14275000
C	19.84876900	37.42853700	39.58707400
O	20.22557300	37.38182000	40.70748400
N	20.52812200	38.07700800	38.55361400
C	21.68509400	38.75981200	38.57432400
C	22.14800900	39.28352600	37.33322500
C	22.46825000	38.95414900	39.76291300
C	23.63750900	39.67031700	39.67798100
C	24.11261100	40.17908000	38.44628600
C	23.32709900	39.93740100	37.26658900
C	25.37901500	40.93152200	38.35715300
C	25.41323200	42.37650100	38.43352000
C	24.50468300	43.24826000	39.28588000
C	25.03098400	44.67790000	39.00332100
N	26.19348700	44.48590300	38.13390600
C	26.41493200	43.14492300	37.95781200
C	27.69399800	42.69815700	37.35235800
C	28.04821100	42.94907200	36.02790300
C	29.27197100	42.50806500	35.53123700
C	30.16394500	41.83412100	36.34292800
C	29.82806500	41.59682300	37.68060400
C	28.60844400	42.02955500	38.17318400
N	31.33374600	41.27578000	35.77184600
C	32.37362000	40.77289500	36.48115300
O	32.71542100	41.16979400	37.57464200
H	27.00468100	45.05760100	38.27740200
H	21.53253600	39.16790100	36.46168100
H	23.68061300	40.31942500	36.32753900
H	24.21046800	39.84743700	40.56649600
H	22.09587500	38.59836600	40.69778000
H	26.25047400	40.34896100	38.60302300
H	24.60078800	42.98245100	40.33346100
H	23.44973100	43.15542800	39.04405400
H	25.32155000	45.18577300	39.91450800
H	24.29073200	45.29121100	38.50245200
H	28.36550700	41.85220400	39.20520200
H	27.37367400	43.47042600	35.37499000
H	29.52457400	42.69005800	34.50137400
H	30.50377200	41.08576800	38.33300500
H	31.27279700	40.99232400	34.81258000
H	20.07480700	38.00814400	37.66703300
H	32.82589000	39.85874000	36.06995500
H	18.92136000	36.92973300	39.26102100

FC STRUCTURE *E*-2-C2

C	34.02402700	40.42924000	32.50363200
C	29.20725600	32.92891600	40.87904700
C	29.51913600	34.25737400	40.26543100
O	28.68251000	35.09806000	40.19851600
N	30.81231000	34.40124000	39.84121200
C	31.41032100	35.61905400	39.47138100
C	32.50436600	35.60365000	38.61600600
C	30.93812100	36.84246300	39.96172400
C	31.58424300	38.01612200	39.61250200
C	32.67387500	38.00918600	38.73043500
C	33.10833300	36.77958100	38.21931900
C	33.29241200	39.25246300	38.30141200
C	33.59919100	40.29605100	39.11572700
C	33.61390900	40.37107700	40.63395100
C	34.55402100	41.55973400	40.91651300
N	34.70892800	42.18990700	39.59148300
C	34.20222200	41.51529500	38.61932600
C	34.26146200	41.93954800	37.21433700
C	33.07219300	41.99640200	36.48957800
C	33.10707200	42.29982200	35.13568200
C	34.33433000	42.50292800	34.51117900
C	35.51340000	42.48101700	35.24988000
C	35.48533400	42.20771800	36.59701200
N	34.39607100	42.76140900	33.11756600
C	34.29774800	41.86486000	32.11214000
O	34.38755400	42.21037700	30.96181900
H	35.10650100	43.10653100	39.45442700
H	32.88873700	34.66014200	38.27671500
H	33.93994600	36.74486500	37.53795800
H	31.19086700	38.94532400	39.97930900
H	30.06682500	36.87726600	40.57544300
H	33.53623100	39.34174100	37.25839000
H	33.98129800	39.45738900	41.08110200
H	32.63208000	40.55446000	41.04678900
H	35.53422900	41.26712100	41.26739400
H	34.15213100	42.28530300	41.60360800
H	36.40489900	42.15758600	37.15215000
H	32.13468900	41.83435700	36.98475600
H	32.19917500	42.35398700	34.56585300
H	36.44329300	42.63180900	34.73891100
H	34.56389800	43.70854900	32.83769400
H	31.38479200	33.58457900	39.81959900
H	34.09688700	40.81137600	32.39942400
H	29.29027300	33.28252800	40.71571400

MINIMUM S_1 *E*-2-C2

C	34.02447817	40.43127887	32.50333138
C	29.20600344	32.93001558	40.88202699
C	29.51506918	34.26400309	40.28318626
O	28.69233947	35.10368231	40.19864208
N	30.83235450	34.42420326	39.83814347
C	31.40735130	35.60248925	39.48162759
C	32.53233087	35.58253994	38.61692980
C	30.91353955	36.85502381	39.96785806
C	31.55445300	38.02156288	39.62208526
C	32.65393617	38.01609465	38.73276872
C	33.10763720	36.74435121	38.22528381
C	33.27885690	39.23706219	38.28515663
C	33.59970372	40.31836367	39.10600311
C	33.63262646	40.38196563	40.62683249
C	34.57944572	41.57606660	40.91195254
N	34.76336731	42.20004703	39.62284748
C	34.18277725	41.50351507	38.61445066
C	34.25915435	41.92157806	37.21817388
C	33.07599975	41.99393512	36.47999688
C	33.10761365	42.29480527	35.12776699
C	34.33546565	42.50164056	34.50680286
C	35.51054672	42.48154287	35.24746393
C	35.47953249	42.20423133	36.59457071
N	34.39744402	42.76073475	33.11065331
C	34.29887948	41.86776320	32.10973725
O	34.38819476	42.20903085	30.95443046
H	35.08585995	43.13702709	39.49236627
H	32.90637250	34.63672066	38.27943380
H	33.93742121	36.73662522	37.54176983
H	31.17941117	38.95666123	39.98652154
H	30.04731738	36.88021015	40.58837268
H	33.53770906	39.30508189	37.24513304
H	33.99379574	39.46782130	41.08261647
H	32.64655431	40.56150289	41.03826103
H	35.53450336	41.24581178	41.30999927
H	34.15618308	42.26880947	41.62597500
H	36.39667571	42.16005009	37.15374850
H	32.13973238	41.83977979	36.98042422
H	32.19916279	42.35628799	34.55896334
H	36.44146731	42.63726148	34.73841559
H	34.56373574	43.70810423	32.83259575
H	31.38863073	33.59417756	39.76541303
H	34.09751894	40.81364557	32.39856359
H	29.28827127	33.28509944	40.72262619

TS S_1 *E*-2-C2			
C	34.02511900	40.43038900	32.50714200
C	29.20011900	32.93370800	40.88414900
C	29.45711100	34.28190200	40.29227300
O	28.61082900	35.10670400	40.26512900
N	30.74405500	34.47651700	39.80962400
C	31.29973300	35.68021000	39.47489100
C	32.41219400	35.66266100	38.59857600
C	30.80832500	36.91770800	39.97658000
C	31.47139100	38.08395400	39.67573700
C	32.57777000	38.08489700	38.76965200
C	32.99054100	36.82162100	38.21089200
C	33.31915100	39.21839700	38.41083900
C	33.57927500	40.41001300	39.21869400
C	33.88516500	40.34810400	40.70158200
C	34.50917800	41.72463600	40.97839400
N	34.90403900	42.19423700	39.65834200
C	34.18831300	41.56108200	38.69242300
C	34.24979100	41.95062600	37.28490200
C	33.07558300	41.94460600	36.52584000
C	33.11187500	42.23387600	35.16879200
C	34.33612500	42.48861300	34.55350200
C	35.50042600	42.53607800	35.31637900
C	35.46327300	42.28445200	36.66755000
N	34.40607000	42.75000100	33.15689200
C	34.30924300	41.87009900	32.13855500
O	34.41252300	42.22849800	30.99104000
H	35.13723500	43.16083100	39.52109600
H	32.78869900	34.71546000	38.26069300
H	33.81494300	36.80988200	37.51932000
H	31.11056700	39.01287300	40.07621300
H	29.93025700	36.93524800	40.58297000
H	33.89635200	39.13118500	37.51429100
H	34.58748700	39.54511400	40.92207400
H	32.99901900	40.17597100	41.30262300
H	35.35370100	41.69419400	41.65287100
H	33.77561000	42.40131900	41.39865500
H	36.37434000	42.30360600	37.23747300
H	32.13786400	41.76496400	37.01574700
H	32.20757800	42.26006700	34.59060800
H	36.43099200	42.74002300	34.82349300
H	34.59775600	43.69474200	32.88475000
H	31.30049100	33.65878100	39.66001300
H	34.10074800	40.81361400	32.40903100
H	29.26852600	33.29257300	40.72660200

(1) Jorgensen, W. L.; Chandrasekhar, J.; Madura, J. D.; Impey, R. W.; Klein, M. L. *J. Chem. Phys.* **1983**, *79*, 926.

(2) Hornak, V.; Abel, R.; Okur, A.; Strockbine, B.; Roitberg, A.; Simmerling, C. *Proteins: Struct., Funct., Bioinf.* **2006**, *65*, 712.

(3) Wang, J.; Wolf, R. M.; Caldwell, J. W.; Kollman, P. A.; Case, D. A. *J. Comput. Chem.* **2004**, *25*, 1157.

(4) Blanco-Lomas, M.; Samanta, S.; Campos, P. J.; Woolley, G. A.; Sampedro, D. *J. Am. Chem. Soc.* **2012**, *134*, 6960.
(5) Singh, U. C.; Kollman, P. A. *J. Comput. Chem.* **1984**, *5*, 129.
(6) Besler, B. H.; Merz, K. M., Jr.; Kollman, P. A. *J. Comput. Chem.* **1990**, *11*, 431.
(7) Becke, A. D. *J. Chem. Phys.* **1993**, *98*, 5648.
(8) Vreven, T.; Byun, K. S.; Komaromi, I.; Dapprich, S.; Montgomery, J. A., Jr.; Morokuma, K.; Frisch, M. J. *J. Chem. Theory Comput.* **2006**, *2*, 815.